PROCEEDINGS OF SCIENCE

Study of finite temperature QCD with 2+1 flavors via Taylor expansion and imaginary chemical potential

Rossella Falcone*
Fakultät für Physik, Universität Bielefeld, D-33615 Bielefeld, Germany
E-mail: rfalcone@physik.uni-bielefeld.de

Edwin Laermann
Fakultät für Physik, Universität Bielefeld, D-33615 Bielefeld, Germany
E-mail: edwin@physik.uni-bielefeld.de

Maria Paola Lombardo
INFN - Laboratori Nazionali di Frascati, I-00044 Frascati (RM), Italy
E-mail: Mariapaola.Lombardo@lnf.infn.it

We study QCD with 2+1 flavors at nonzero temperature and nonzero chemical potential. We present preliminary results obtained from lattice calculations performed with an improved staggered fermions action (p4-action) on lattice with temporal extent $N_t = 4$ on a line of constant physics with the strange quark mass adjusted to its physical value and a pion mass of about 220 MeV. We compute at imaginary chemical potential and compare with Taylor expansion results. We focus our study on a range of temperatures $0.94 < T/T_c < 1.08$.

The XXVIII International Symposium on Lattice Field Theory, Lattice2010
June 14-19, 2010
Villasimius, Italy

*Speaker.

© Copyright owned by the author(s) under the terms of the Creative Commons Attribution-NonCommercial-ShareAlike Licence.

PoS(Lattice 2010)183

1. Introduction

Understanding the phase diagram of QCD in the temperature - chemical potential (T,μ) plane is crucial for many implications in astrophysics, cosmology and in the phenomenology of heavy-ion collisions. While the lattice formulation of QCD provided fruitful information at finite temperature, at non-vanishing chemical potential lattice simulations suffer from the sign problem. Only in recent years several different methods [1, 2, 3, 4, 5, 6, 7] have been devised to at least partly overcome this obstacle.

In this work we present results from lattice calculations in QCD with dynamical light and strange quark degrees of freedom at non zero temperature and imaginary chemical potential. Our calculations are performed with a tree level Symanzik-improved gauge action and an improved staggered fermion action, the p4-action with 3-link smearing (p4fat3) [8]. We focus on a range of temperatures in the vicinity of the pseudocritical temperature T_c at vanishing chemical potential, $0.94 < T/T_c < 1.08$. At each temperature we carried out simulations on lattices with temporal extent $N_t = 4$. Following [9], at each temperature the strange quark mass was adjusted to its physical value and the light up and down quark masses were taken to be degenerate and equal to $m_s/10$, which corresponds to a constant Goldstone pion mass of about 220 MeV. This allows us to utilize the zero temperature results and interpolations of [9] for the conversion of lattice parameters into physical units. For definiteness, we apply a value of $T_c = 202$ MeV for the pseudocritical temperature at zero density. To insure small finite volume effects the spatial volume has been chosen to be $V^{1/3}T = 4$. The number of gauge field configurations analyzed varies from 1000 to 2000, the configurations are separated by 10 trajectories. All numerical simulations have been performed using the Rational Hybrid Monte Carlo (RHMC) algorithm [10, 11].

At each temperature we performed calculations at several values of the imaginary quark chemical potential, $\mu_q = i\mu_I, q = u,d,s$ which was taken to be degenerate for all three flavors. In the following, we first present results relevant for an estimate of the pseudocritical line in the (T,μ_I) plane and then compare our findings at imaginary chemical potential with results obtained within the Taylor expansion approach.

2. The pseudocritical line at imaginary chemical-potential

At imaginary chemical potential and high temperature, the phase diagram of QCD features the Roberge Weiss transition at $\mu_I^c = \pi T/3$, associated with the phase of the Polyakov loop. The line of Roberge Weiss transitions ends at $T = T_{RW}$. At lower temperature the 'quark-gluon plasma' region is limited by a chiral transition [3, 4] which continues to real values of μ. In this work we focus our study on the range of temperatures $0.94 < T/T_c < 1.08$, i.e. to the vicinity of the pseudocritical temperature T_c at zero density.

In order to study the phase structure of QCD in the (T,μ_I) plane, it is very useful [4] to consider the phase of the Polyakov loop, $L(x)$, that we can parameterize as $L(x) = |L(x)|e^{i\phi}$. In the presence of dynamical fermions and with imaginary chemical potential we expect $\langle\phi\rangle = -\theta$ at low temperatures ($\theta \equiv \mu_I/T$), and $\langle\phi\rangle \sim 2k\pi/3$ for $(k-1/2) < \frac{3}{2\pi}\theta < (k+1/2)$ at high temperatures; the values $\theta = 2(k+1/2)\pi/3$ correspond to the Roberge Weiss transitions from one Z_3 sector to the other. In Fig. 1 we show our results for $\langle\phi\rangle$ versus the imaginary chemical potential for different

PoS(Lattice 2010)183

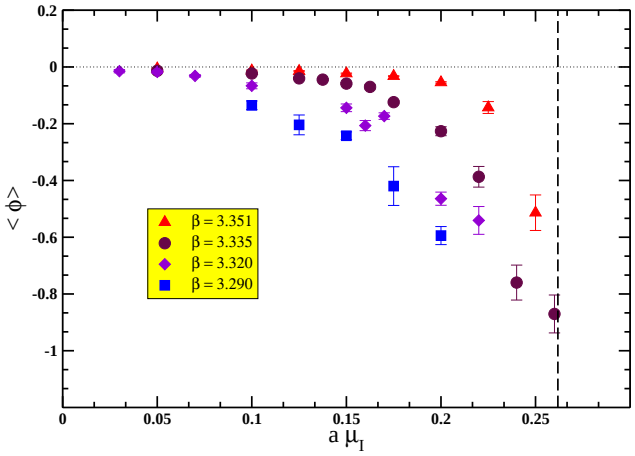

Figure 1: The Polyakov loop phase $\langle\phi\rangle$ as a function of the imaginary chemical potential for 4 different beta values. The vertical dashed line corresponds to the RW transition at $a\mu_I^c = \pi/3N_t$.

values of temperatures. For $\beta = 3.290$ which is below the critical value at $\mu_I = 0$ we found that $\langle\phi\rangle$ starts to deviate from zero right away at non vanishing potential. For the β values above the critical one we observe that $\langle\phi\rangle$ stays close to 0 until a certain temperature dependent value of $a\mu_I$ is reached where the Polyakov loop phase begins to decrease with increasing μ_I. We will take that value as an estimate for the location of the pseudocritical chiral line [4]. A jump of the phase is not observed at any temperature which indicates that all our T values are below T_{RW}

In Fig. 2 we display our results for the modulus of the Polyakov loop and the light quark chiral condensate as functions of the imaginary chemical potential for $\beta = 3.320, 3.335, 3.351$ which correspond to temperatures of 204.8 MeV, 209.6 MeV and 218.2 MeV respectively [9]. The chiral condensate is defined as

$$\langle\hat{\psi}\psi\rangle_q \equiv \frac{1}{4}\frac{1}{N_\sigma^3 N_t}\langle TrM^{-1}(m_q)\rangle, \quad q = u,d,s \tag{2.1}$$

where N_σ^3 is the spatial volume and M the fermionic matrix. In the same figure we also display the behavior of the Polyakov loop susceptibility

$$\chi_L = N_\sigma^3\left(\langle L^2\rangle - \langle L\rangle^2\right) \tag{2.2}$$

as a function of μ_I, for the same beta values. In the upper row of Fig. 2 we indicate by vertical lines the estimates for the critical μ_I values and their errors as obtained from the phase of the Polyakov loop. It is seen, most clearly at the largest temperature investigated, that in the region where the Polyakov phase starts to deviate from 0 also the chiral condensate exhibits a rise while the modulus of the Polyakov loop decreases.

Based on the estimates for the pseudocritical μ_I values, to leading order in μ/T the critical line can be parameterized as

$$\frac{T_c(\mu)}{T_c} = 1 - t_2(N_f, m_f)\left(\frac{\mu}{\pi T}\right)^2 + \mathscr{O}\left(\left(\frac{\mu}{\pi T}\right)^4\right) \tag{2.3}$$

PoS(Lattice 2010)183

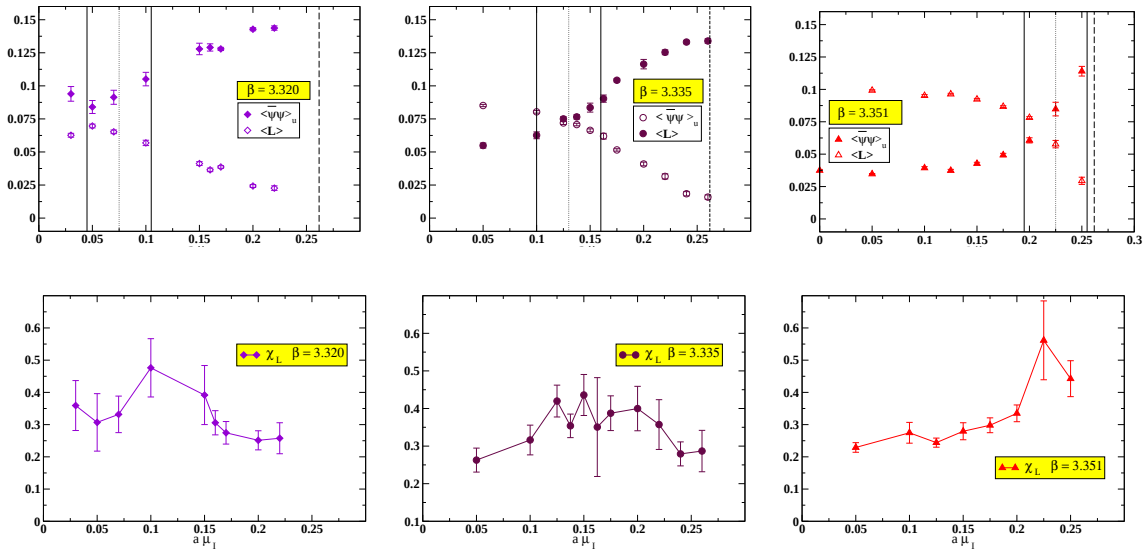

Figure 2: Chiral condensate and Polyakov loop as functions of the imaginary chemical potential (upper row) for beta values above the critical value. The vertical dashed line corresponds to the RW transition, the vertical continuous ones to the estimation of the critical μ_I from the Polyakov loop phase; (lower row) Polyakov loop susceptibility as function of μ_I for the same beta values.

where T_c is the critical temperature at zero chemical potential. The coefficient of the leading term, t_2, has been calculated for various cases, see the collection in [12]. In Fig. 3 (left) we compare our data points on $T_c(\mu)/T_c$ with results which have been obtained from reweighting simulations at $\mu = 0$ within the same discretization scheme as ours. In [6] two rather heavy quark flavors were taken into account whereas in [14] the number of flavors was 3, with similar masses as in our case. Although the error bars are large the comparison suggests that the curvature t_2 grows with N_f which is consistent with a behavior $\sim N_f/N_c$ found in large N_c expansion [15]. In Fig. 3 (right) we show our results fit. We checked the stability of the fit by choosing different ranges in the chemical potential values. Considering the entire range of values we find $t_2 = 0.89(4)$, discarding the first value we find $t_2 = 0.89(5)$ and discarding the last one, $t_2 = 1.02(12)$.

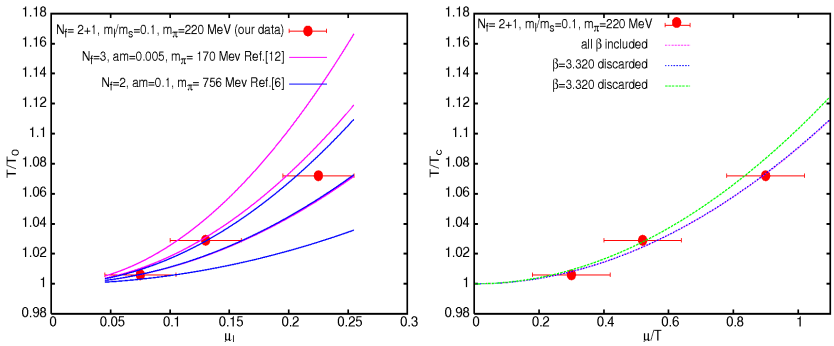

Figure 3: The pseudocritical line at imaginary μ: comparison between our data points and results from the literature [6, 14] (left); our fit results (right).

PoS(Lattice 2010)183

3. The quark number density at imaginary chemical potential

For a large homogeneous system, the pressure and its first derivatives, the quark number densities, are defined as

$$\frac{p}{T^4} = \frac{1}{VT^3} \ln \mathscr{Z} \tag{3.1}$$

$$\frac{n_{u,d,s}}{T^3} = \frac{1}{VT^2} \frac{\partial \ln \mathscr{Z}}{\partial \mu_{u,d,s}} \tag{3.2}$$

where the partition function $\mathscr{Z}$ is a function of the volume V, temperature T, quark masses $m_{u,d,s}$ and chemical potentials $\mu_{u,d,s}$. Note that for imaginary chemical potential the quark number density is purely imaginary [16].

We calculated the quark number density at various values of the imaginary chemical potential $\mu = i\mu_I$. In Fig. 4 (left) we show our results for the light, n_l, $l = u,d$, and the strange quark number density, n_s, at the temperature $T = 209.6$ MeV. We fitted our data to the ansatz

$$\Im\, n(\mu_I) = A\mu_I(c^2 - {\mu_I}^2)^e \tag{3.3}$$

which was suggested in [17]. This ansatz takes into account that the quark number density is an odd function of the chemical potential. Moreover, if the exponent e is less than 1, Eq. 3.3 leads to a singularity in the quark number susceptibility at c. Eq. 3.3 can also be derived from the singular part of the $ln\mathscr{Z}$ in the vicinity of a critical point $c = \mu_I^c$, with e given by the critical exponent α as $e = 1 - \alpha$. In Fig. 4 (right) we show the results of the fit to the light quark density obtained at a temperature of 209.6 MeV. A fit to our entire interval and with c unconstrained gives $A = 105(67)$, $c = 0.285(14)$ and $e = 1.30(28)$. In the range $[0.15, 0.26]$ of $a\mu_I$, we obtain $A = 57(54)$, $c = 0.276(15)$ and $e = 1.06(36)$. We thus find that e is consistent with 1 and substantially larger than the value $0.28(2)$ found in [17] while c exceeds $\pi T/3$ slightly. We interpret these results as to indicate that the regular contributions to $ln\mathscr{Z}$ are dominating the number density at the temperatures investigated (see also [13]).

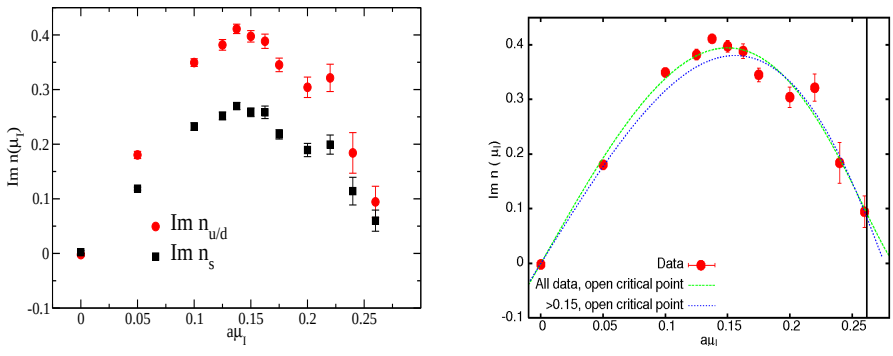

Figure 4: (left) n_l and n_s in comparision; (right) quark number density n_l at T=209.6 MeV fitted to the form predicted by a simple critical behavior at imaginary chemical potential. The vertical line indicates the Roberge Weiss transition.

PoS(Lattice 2010)183

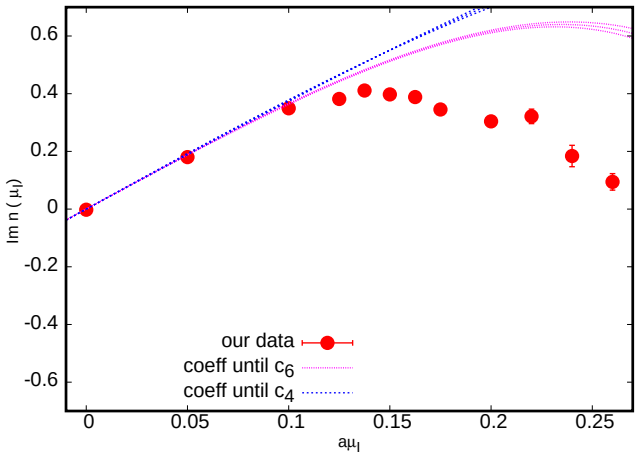

Figure 5: The light quark number density at 209.6 MeV calculated at imaginary chemical potentials (points) and from Taylor expansion (curves with error bands). The pink curve from [18] takes into account coefficients up to 6th order. The blue curve has been obtained from our own computations of the coefficients until fourth order which have less statistics.

One of the approaches to QCD at finite density is based on the Taylor expansion of the pressure in terms of the quark chemical potentials around a generic $\mu_0 = (\mu_{u,0}, \mu_{d,0}, \mu_{s,0})$,

$$\frac{p}{T^4}(\hat{\mu}) = \sum_{k,l,n} c_{kln}(\hat{\mu}_u - \hat{\mu}_{u,0})^k(\hat{\mu}_d - \hat{\mu}_{d,0})^l(\hat{\mu}_s - \hat{\mu}_{s,0})^n \tag{3.4}$$

with the abbreviation $\hat{\mu}_q = \mu_q/T$ and the coefficients

$$c_{kln} = \frac{1}{k!l!n!}\frac{\partial^k}{\partial\hat{\mu}_u{}^k}\frac{\partial^l}{\partial\hat{\mu}_d{}^l}\frac{\partial^n}{\partial\hat{\mu}_s{}^n}\left(\frac{p}{T^4}\right) \tag{3.5}$$

evaluated at μ_0. Correspondingly, the number density of e.g. the u quark is given by

$$\frac{n_u}{T^3}(\hat{\mu}) = \sum_{k,l,n} k c_{kln}(\hat{\mu}_u - \hat{\mu}_{u,0})^{k-1}(\hat{\mu}_d - \hat{\mu}_{d,0})^l(\hat{\mu}_s - \hat{\mu}_{s,0})^n. \tag{3.6}$$

Usually the coefficients are computed at $\mu_{q,0} = 0$ but they could also be calculated at imaginary values for the chemical potentials. This is work in progress.

In Fig. 5 we compare our data for the quark number density calculated at imaginary chemical potentials with predictions from the Taylor expansion at a temperature of 209.6 MeV and at the same lattice parameters. Up to $\mu_I/T \simeq 0.4$ there is practically no difference between the predictions obtained from Taylor expansion up to fourth and 6th order [18]. At larger values of μ_I the 6th order Taylor curve starts to deviate from the fourth order one and bends downwards, thus qualitatively describing this trend of the data correctly. Still, the errors arising from truncanting the Taylor series at sixth order become sizeable at $\mu_I/T \simeq 0.4$ at this temperature.

4. Summary and conclusions

We have studied QCD with 2+1 flavors at nonzero temperature and nonzero chemical potential on a line of constant physics with the strange quark mass adjusted to its physical value and the pion

PoS(Lattice 2010)183

mass of about 220 MeV. The simulations have been carried out at imaginary chemical potentials. It turned out that the temperatures of up to $1.08T_c$ at which the computations were performed are below the endpoint T_{RW} of a line of Roberge Weiss transitions. Instead, we could identify a crossover line at which phase and modulus of the Polyakov loop as well as the chiral condensate change their behavior. The curvature of this line was estimated as $t_2 = 0.89(2)$ which is not inconsistent with the literature. Furthermore, we calculated quark number densities at imaginary μ and compare our data with results obtained via Taylor expansion method. Up to $\mu_I/T \simeq 0.4$ good agreement was observed.

Acknowledgments

This work has been supported in parts by the BMBF grant 06BI9001 and the EU Integrated Infrastructure Initiative "Hadron Physics 2". The numerical simulations have been performed on the apeNEXT at Bielefeld University.

References

[1] I. M. Barbour *et al.*, *Nucl.Phys.Proc.Suppl* **60A** (1998) 220, [hep-lat/9705042]

[2] Z. Fodor and S.D. Katz, *Phys.Lett* **B534** (2002) 87, [hep-lat/0104001]

[3] Ph. de Forcrand, O. Philipsen, *Nucl.Phys.* **B642** (2002) 290, [hep-lat/0205016]

[4] M. D'Elia, M.P. Lombardo, *Phys.Rev.* **D67** (2003) 014505, [hep-lat/0209146]

[5] R.V. Gavai, S. Gupta, *Phys.Rev.* **D68** (2003) 034506, [hep-lat/0303013]

[6] C.R. Allton *et al.*, *Phys.Rev.* **D66** (2002) 074507, [hep-lat/0204010]

[7] Ph. de Forcrand, S. Kratochvila, *Nucl. Phys.* **B** (Proc. Suppl.) **153** (2006) 62, [hep-lat/0602024]

[8] F. Karsch, E. Laermann and A. Peikert, *Phys.Lett.* **B478** (2000) 447, [hep-lat/0002003]

[9] M. Cheng *et al.*, *Phys.Rev* **D77** (2008) 014511, [arxiv:0710.0354]

[10] I. Horváth, A.D. Kennedy and S. Sint, *Nucl.Phys.Proc.Suppl.* **73**, (1999) 834, [hep-lat/0608016];
M.A. Clark, A.D. Kennedy and Z. Sroczynski, *Nucl.Phys.Proc.Suppl.* **140**, (2005) 835, [hep-lat/0409133]

[11] M. Cheng *et al.*, *Phys.Rev.* **D75**, (2007) 034506, [hep-lat/0612001]

[12] C. Schmidt, PoS **LAT2006** 021, [hep-lat/0610116]

[13] C. Schmidt, PoS **CPOD2009** 024, [arxiv:0910.4321]

[14] F. Karsch *et al.*, *Nucl.Phys.Proc.Suppl.* **129** (2004) 614, [hep-lat/0309116]

[15] D. Toublan, [hep-th/0510090]

[16] M. D'Elia, M.P. Lombardo, *Phys.Rev.* **D70** (2004) 074509, [hep-lat/0406012]

[17] M. D'Elia, F. Di Renzo, M.P. Lombardo, *Phys.Rev.* **D76** (2007) 114509, [arxiv:0705.3814]

[18] M. Cheng *et al.*, *Phys.Rev.* **D79** (2009) 074505, [arXiv:0811.1006]

PoS(Lattice 2010)183